Open access • Posted Content • DOI:10.1101/360909

The age-dependent relationship between resting heart rate variability and functional brain connectivity — Source link

Deniz Kumral, Deniz Kumral, Herma Lina Schaare, Frauke Beyer ...+19 more authors

Institutions: Humboldt University of Berlin, Max Planck Society, Leipzig University, Dresden University of Technology

Published on: 03 Jul 2018 - bioRxiv (Cold Spring Harbor Laboratory)

The age-dependent relationship between resting heart rate variability and functional brain connectivity

D. Kumral[1,2], H.L. Schaare[1,3], F. Beyer[1,4], J. Reinelt[1], M. Uhlig[1,3], F. Liem[1], L. Lampe[1], A. Babayan[1], A. Reiter[5,1], M. Erbey[2], J. Roebbig[1], M. Loeffler[6], M.L. Schroeter[1,6,7], D. Husser[8], A.V. Witte[1], A. Villringer[1,2,4,6,9], M. Gaebler[1,2,6]

[1] Department of Neurology, Max Planck Institute for Human Cognitive and Brain Sciences, Leipzig, Germany

[2] MindBrainBody Institute at the Berlin School of Mind and Brain, Humboldt-Universitaet zu Berlin, Berlin, Germany

[3] International Max Planck Research School NeuroCom, Leipzig, Germany

[4] Subproject A1, Collaborative Research Centre 1052 “Obesity Mechanisms”, University of Leipzig, Leipzig, Germany

[5] Lifespan Developmental Neuroscience, Technical University of Dresden, Dresden, Germany

[6] LIFE – Leipzig Research Center for Civilization Diseases, University of Leipzig, Leipzig, Germany

[7] Department of Cognitive Neurology, University of Leipzig, Leipzig, Germany

[8] Department of Electrophysiology, Leipzig Heart Centre, University of Leipzig, Leipzig, Germany

[9] Center for Stroke Research Berlin, Charité – Universitaetsmedizin Berlin, Berlin, Germany

Abstract

Resting heart rate variability (HRV), an index of parasympathetic cardioregulation and an individual trait marker related to mental and physical health, decreases with age. Previous studies have associated resting HRV with structural and functional properties of the brain – mainly in cortical midline and limbic structures. We hypothesized that HRV may alter its relationship with brain structure and function across the adult lifespan. In 388 healthy subjects of three age groups (140 younger: 26.0±4.2 years, 119 middle-aged: 46.3±6.2 years, 129 older: 66.9±4.7 years), gray matter structure (voxel-based morphometry) and resting-state functional connectivity (eigenvector centrality mapping and exploratory seed-based functional connectivity) were related to resting HRV, measured as the root mean square of successive differences (RMSSD). Confirming previous findings, resting HRV decreased with age. For HRV-related gray matter volume, there were no statistically significant differences between the age groups, nor similarities across all age groups. In whole-brain functional connectivity analyses, we found an age-dependent association between resting HRV and eigenvector centrality in the bilateral ventromedial prefrontal cortex (vmPFC), driven by the younger adults. Across all age groups, HRV was positively correlated with network centrality in bilateral posterior cingulate cortex. Seed-based functional connectivity analysis using the vmPFC cluster revealed an HRV-related cortico-cerebellar network in younger but not in middle-aged or older adults. Our results indicate that the decrease of HRV with age is accompanied by changes in functional connectivity along the cortical midline. This extends our knowledge of brain-body interactions and their changes over the lifespan.

Keywords: heart rate variability, aging, eigenvector centrality mapping, brain structure, voxel-based morphometry, default mode network

1. Introduction

Behavioral and physiological changes that occur with advancing age become manifest in the structure and function of multiple macro- and micro-systems of the human organism (Arking, 2006). Important alterations occur in the cardiovascular and the nervous systems, which are coupled to react dynamically to environmental demands (McEwen, 2003). Such adaptations to internal and external challenges, while leaving an imprint on body and brain, underlie healthy aging (Lipsitz and Goldberger, 1992; Swank, 1996). They are also reflected in brain-heart interactions – particularly in parasympathetic cardioregulation – that can be measured as resting heart rate variability (HRV)

HRV quantifies variations in the cardiac beat-to-beat (or RR) interval that can be measured with an electrocardiogram (ECG). Phasic modulation of the heart rate arises from the influences of both branches of the autonomic nervous system (ANS), the parasympathetic (PNS) and the sympathetic nervous system (SNS) – with the PNS quickly lowering the heart rate and the SNS slowly increasing it. Because the PNS has very short response latencies, HRV – and some HRV measures more than others – represents parasympathetic (i.e., vagal) influences on the heart (Thayer and Lane, 2007). HRV, typically acquired at rest, is known to decrease with age (De Meersman and Stein, 2007; Umetani et al., 1998). Preservation of autonomic function, as indexed by relatively increased HRV, has been shown a prerequisite for longevity and healthy aging (Zulfiqar et al., 2010). Higher HRV has also been associated with higher health (Kemp and Quintana, 2013) – for example, with less cardiovascular diseases (Liao et al., 1997; Thayer et al., 2010) – and reduced overall mortality (Buccelletti et al., 2009). In older adults, HRV can indicate inter-individual differences in cognitive performance (Mahinrad et al., 2016; Zeki Al Hazzouri et al., 2014). Hence, resting HRV could be regarded as a biomarker of healthy aging.

The neurovisceral integration model considers the role of the brain in parasympathetic cardioregulation and provides a framework to explain individual differences in resting vagal function (Kemp et al., 2017; Thayer et al., 2012). According to this model, frontal and midbrain areas interact and the prefrontal cortex (PFC) inhibits subcortical regions as well as the ANS. Thereby, the heart is under tonic inhibitory control by the ANS. Assuming this close interaction of the brain and the ANS in heart rate regulation, it has been suggested that inter-individual differences in HRV may reflect structural and functional variability in the brain (Thayer et al., 2012). Indeed, inter-individual differences in resting HRV have been associated with cortical thickness in right anterior midcingulate cortex (aMCC) (Winkelmann et al., 2017) as well as in rostral anterior cingulate cortex (ACC) and left lateral orbitofrontal cortex (OFC) (Yoo et al., 2017). A recent study in individuals between 20 and 60 years found a negative correlation between resting HRV and gray matter volume in limbic structures like insula, amygdala, and parahippocampal gyrus (Wei et al., 2018). Similar brain regions have also been related to HRV in functional neuroimaging studies (Holzman and Bridgett, 2017; Mather and Thayer, 2018; Thayer et al., 2012); both task-based (e.g., BOLD: Critchley et al., 2000; regional cerebral blood flow; rCBF: Gianaros et al., 2004; meta-analyses: Beissner et al., 2013; Thayer et al., 2012) and under resting state conditions (Chang et al., 2013; Jennings et al., 2016; Sakaki et al., 2016). In these studies, activation and connectivity in the medial prefrontal cortex (mPFC), anterior cingulate cortex (ACC), and posterior cingulate cortex (PCC) have most consistently been associated with HRV. These brain areas involved in parasympathetic cardioregulation overlap with the default mode network (DMN) and particularly its nodes along the cortical midline (Beissner et al., 2013). However, the only fMRI study that investigated heart-brain interactions across the adult lifespan included 17 younger and 18 older subjects and restricted their analyses to *a priori* defined regions-of-interest (Sakaki et al., 2016). Across all subjects, higher HRV was related to stronger

functional connectivity between right amygdala and medial prefrontal regions, while age group differences were found in HRV-related connectivity between right amygdala and lateral prefrontal regions.

We here investigated brain-heart interactions across the adult lifespan by combining measures of brain structure and function with the assessment of resting HRV. The main aims of this study were to examine (i) the relationship between resting HRV, brain structure, and functional connectivity as well as (ii) its dependence on age in a large sample of healthy adults across the lifespan. Based on previous findings (reviewed above), we hypothesized that inter-individual differences in the brain correlate with inter-individual differences in resting HRV and that this correlation changes with age. To detect HRV-related structural alterations, we used voxel-based morphometry (VBM) (Ashburner and Friston, 2000). To assess HRV-related changes in the functional architecture across the whole brain, we used the graph-based method of eigenvector centrality mapping (ECM). ECM can identify important network nodes (in this case: voxels) based on their functional connectivity (similar to Google's page rank algorithm) and without the need of an *a priori* selection of a specific seed region or the number of networks / components (Lohmann et al., 2010; Wink et al., 2012). To further explore ECM-derived whole-brain connectivity patterns, we also implemented a resting-state seed-based connectivity analysis (for more details see *Methods*).

2. Methods

2.1.Participants

Data from two studies were used: (I) the Leipzig Research Centre for Civilization Diseases (LIFE; Loeffler et al., 2015) and (II) the "Leipzig Study for Mind-Body-Emotion Interactions" (LEMON; Babayan et al., under review).

LIFE is a large population-based cohort study from Leipzig, Germany (Loeffler et al., 2015). From the sample of LIFE subjects with MRI data (n = 2,667), we selected healthy subjects between the ages of 20 and 80 years. We applied strict exclusion criteria in three categories: I) health-related criteria; participants were excluded if they reported any medication intake except vitamin food supplements, any past or present cardiovascular health problems and diagnoses, or surgeries, any other medical history and/or diagnosis, in a medical interview. II) ECG-related criteria (see details on ECG acquisition below); if a subject had more than one ECG recording, we used the first acquired ECG file that was collected on the same day as the MRI acquisition. Otherwise, we selected the ECG recording that was temporally closest to MRI acquisition. Regarding data quality, we excluded data with unrepairable signal artifacts or problems regarding R-peak detection. We also omitted data with any abnormal ECG signal (e.g., supraventricular extrasystoles) after visual inspection as well as subjects with extreme HRV values based on Tukey's (1977) criterion of 3 interquartile ranges (IQR) above the LIFE sample median (N=14, *Median*: 30.13, IQR: 29.76). III) MRI-related criteria; we excluded subjects with incidental findings (e.g., brain tumor, multiple sclerosis, or stroke) on T1-weighted and/or fluid-attenuated inversion recovery (FLAIR) images. We further excluded subjects based on rs-fMRI quality assessment, for example with faulty preprocessing (e.g., during denoising) or excessive head motion (criterion: mean framewise displacement (FD) > 0.6 mm; Power et al., 2012).

LEMON is a cross-sectional sample of healthy younger and older subjects from Leipzig, Germany, who had never participated in another "psychological or MRI research"-related study, did not report any neurological disorders, head injury, any medication affecting the cardiovascular and/or central nervous system, alcohol or other substance abuse, hypertension, pregnancy, claustrophobia, chemotherapy and malignant diseases, current and/or previous psychiatric disease (Babayan et al., under review). The LEMON sample comprised 171 eligible subjects divided into two age groups (young: 20-35 years, old: 59-75 years). Similar to the exclusion criteria mentioned above, subjects with incomplete data (N = 38), incidental findings in MRI (FLAIR, T2-weighted, T1-weighted, SWI) (N=7), or psychoactive drug intake (e.g., tetrahydrocannabinol) determined by urine test (N = 9) were excluded. Two subjects were discarded due to the HRV outlier criterion mentioned above (LEMON sample *Median*: 40.62, IQR: 39.82) and five subjects due to excessive head motion (mean FD > 0.6 mm; Power et al., 2012). To increase the statistical power and the comparability, we pooled the two samples and divided them into three age groups: young (20-35 years from LIFE and LEMON), middle-aged (35-60 years from LIFE), and old (60-80 years from LIFE and LEMON). Details are provided in Table 1.

Both studies were in agreement with the Declaration of Helsinki and approved by the ethics committee of the medical faculty at the University of Leipzig, Germany.

2.2.ECG collection and HRV analysis

LIFE sample. Ten seconds of a standard medical 12-lead resting ECG were acquired using a Page-Writer TC50 ECG system (Philips Medical Systems, Amsterdam, Netherlands) in supine position. We used lead I (from Einthoven's triangle) for the analysis. R-peaks were automatically detected using the findpeaks function in Matlab 9 (The MathWorks, Inc., Natick, Massachusetts) or Kubios 2.2 (Tarvainen et al., 2014). The ECG data for each subject was manually checked for physiological or computational artifacts like supraventricular

extrasystoles or faulty peak detection, respectively. From RR interval time series (i.e., tachograms), we calculated the root mean square of successive differences (RMSSD) of adjacent RR intervals (Task Force of the European Society of Cardiology and the North American Society of Pacing Electrophysiology, 1996).

LEMON sample. Four minutes of resting ECG were acquired using a Biopac MP35 amplifier with the acquisition software AcqKnowledge version 4.0 (Biopac Systems Inc., http://www.biopac.com, Goleta, CA, USA) and three disposable electrodes on the thorax: the reference electrode was attached near the right collarbone, the measuring electrode on the left-hand side of the body on the same level as the 10th rib, and the ground electrode on the right hip bone. The subjects were instructed to think about daily routines, relax, and breathe at a comfortable rate in sitting position. The peak detection and RMSSD calculation were performed using Kubios 2.2 (Tarvainen et al., 2014).

RMSSD values of our sample were natural log-transformed to obtain normally distributed data (Shapiro-Wilk tests; $W = 0.99$, $p = 0.12$). In the rest of the paper, log-transformed RMSSD will be referred to as "HRV".

2.3.MRI acquisition

Brain imaging for both datasets was performed on the same 3T Siemens Magnetom Verio MR scanner (Siemens Medical Systems, Erlangen, Germany) with a standard 32-channel head coil. In both samples, subjects were instructed to keep their eyes open and not to fall asleep during the acquisition period.

LIFE sample. The structural T1-weighted images were acquired using a generalized auto-calibrating partially parallel acquisition technique (Griswold et al., 2002) and the Alzheimer's Disease Neuroimaging Initiative standard protocol with the following parameters: inversion time (TI) = 900 ms, repetition time (TR) = 2.3 ms, echo time (TE) = 2.98 ms, flip angle (FA) = 9°, band width = 240 Hz/pixel, field of view (FOV) = 256 x 240 x

187 176 mm^3, voxel size = 1 x 1 x 1 mm^3, no interpolation. T2*-weighted functional images were
188 acquired using an echo-planar-imaging (EPI) sequence with the following parameters: TR =
189 2000 ms, TE= 30 ms, FA = 90°, FOV = 192 x 192 x 144 mm^3, voxel size = 3 mm x 3 mm,
190 slice thickness = 4 mm, slice gap = 0.8 mm, 300 volumes, duration = 10.04 min. A gradient
191 echo field map with the sample geometry was used for distortion correction (TR = 488 ms,
192 TE 1 = 5.19 ms, TE 2 = 7.65 ms).
193 *LEMON sample.* The structural image was recorded using an MP2RAGE sequence
194 (Marques et al., 2010) with the following parameters: TI 1 = 700 ms, TI 2 = 2500 ms, TR =
195 5000 ms, TE = 2.92 ms, FA 1 = 4°, FA 2 = 5°, band width = 240 Hz/pixel, FOV = 256 × 240
196 × 176 mm^3, voxel size = 1 x 1 x 1 mm^3. The functional images were acquired using a T2*-
197 weighted multiband EPI sequence with the following parameters: TR = 1400 ms, TE = 30 ms,
198 FA= 69°, FOV = 202 mm, voxel size = 2.3 x 2.3 x 2.3 mm^3, slice thickness = 2.3 mm, slice
199 gap = 0.67 mm, 657 volumes, multiband acceleration factor = 4, duration = 15.30 min. A
200 gradient echo field map with the sample geometry was used for distortion correction (TR =
201 680 ms, TE 1 = 5.19 ms, TE 2 = 7.65 ms).
202 2.4.MR data preprocessing and analysis
203 *Structural MRI.* We analyzed structural brain alterations on the T1-weighted 3D image
204 using VBM (Ashburner and Friston, 2000) as implemented in SPM12 (Wellcome Trust
205 Centre for Neuroimaging, UCL, London, UK) and the Computational Anatomy Toolbox
206 (CAT12: http://dbm.neuro.uni-jena.de/cat/), running on Matlab 9.3 (Mathworks, Natick, MA,
207 USA). In the LEMON sample before the preprocessing, we removed the background noise
208 from MP2RAGE on the computed uniform images via masking (Streitbürger et al., 2014).
209 The preprocessing steps consisted of segmentation, bias-correction, and normalization using
210 high-dimension Diffeomorphic Anatomical Registration Through Exponentiated Lie Algebra
211 (DARTEL; Ashburner, 2007) with the template from 550 healthy controls of all ages in the

IXI Dataset (http://www.brain-development.org) in MNI space. We then applied a 12-parameter affine registration and nonlinear transformation to correct for image size and position. The voxel size was resampled to 1.5 × 1.5 × 1.5 mm and smoothed using a 8-mm Gaussian kernel. For each subject, whole-brain gray matter volume (GMV) was calculated. An absolute threshold mask of 0.05 was specified in the analyses to cover the whole brain. For quality assessment, we visually inspected the segmentation quality and image homogeneity with the CAT12 toolbox. One participant from the middle-aged group was excluded because of MRI inhomogeneities.

Functional MRI. Preprocessing was implemented in Nipype (Gorgolewski et al., 2011), incorporating tools from FreeSurfer (Fischl, 2012), FSL (Jenkinson et al., 2012), AFNI (Cox, 1996), ANTs (Avants et al., 2011), CBS Tools (Bazin et al., 2014), and Nitime (Rokem et al., 2009). The pipeline comprised the following steps: (I) discarding the first five EPI volumes to allow for signal equilibration and steady state, (II) 3D motion correction (FSL mcflirt), (III) distortion correction (FSL fugue), (IV) rigid body co-registration of functional scans to the individual T1-weighted image (Freesurfer bbregister), (V) denoising including removal of 24 motion parameters (CPAC, Friston et al., 1996), motion, signal intensity spikes (Nipype rapidart), physiological noise in white matter and cerebrospinal fluid (CSF) (CompCor; Behzadi et al., 2007), together with linear and quadratic signal trends, (VI) band-pass filtering between 0.01-0.1 Hz (Nilearn), (VII) spatial normalization to MNI152 standard space (3 mm isotropic) via transformation parameters derived during structural preprocessing (ANTS). (VIII) The data were then spatially smoothed with a 6-mm FWHM Gaussian kernel.

The reproducible workflows containing all implementation details for our datasets can be found here: LIFE; https://github.com/fliem/LIFE_RS_preprocessing, LEMON; https://github.com/NeuroanatomyAndConnectivity/pipelines/releases/tag/v2.0

236 *Eigenvector Centrality Mapping (ECM).* In ECM, each voxel in the brain receives a
237 centrality value that is larger if the voxel is strongly correlated with many other voxels that
238 are themselves central (Lohmann et al., 2010). ECM is computationally efficient, enables
239 connectivity analysis at the voxel level, and does not require initial thresholding of
240 connections (Lohmann et al., 2010). Here, the fast ECM implementation was used (Wink et
241 al., 2012). We restricted our ECM analysis to GM, which we extracted with a mask from the
242 tissue priors in SPM12 by selecting voxels with a GM tissue probability of 20% or higher.
243 The resulting mask contained ~63,000 voxels covering the entire brain.
244 *Exploratory Seed-based Functional Connectivity Analysis (SBCA).* To further explore
245 the connectivity patterns of significant centrality changes across the whole brain, ECM was
246 complemented by SBCA. Regions detected in ECM can be used as seeds in a subsequent
247 SBCA to investigate intrinsic functional connectivity patterns (Taubert et al., 2011). A
248 bilateral vmPFC seed was created by binarizing the significant ECM findings (MNI
249 coordinates: [x=0, y=57, z=-6], cluster size k=62). Time series were extracted and averaged
250 across all voxels of the seed. For each subject, a correlation between the time series of the
251 seed and every other voxel in the brain was calculated using 3dfim+ (AFNI). The resulting
252 correlation maps were Fisher r-to-z transformed using 3dcalc (AFNI).
253 *Statistical analyses.* Statistical analyses were carried out using the general linear model
254 (GLM) approach implemented in SPM12. We performed one-way ANOVA with three age
255 groups (young, middle, and old) as between-subjects factor together with HRV as the variable
256 of interest and age, sex, study, and either total intracranial volume (TIV, for VBM analysis) or
257 in-scanner head motion (mean FD; Power et al., 2012 for ECM and SBCA) as covariates of
258 no interest.
259 We first calculated the interaction effect between HRV and age group. Based on the
260 significant results of the ANOVA, we computed pairwise group differences using

independent t-tests. Using one-sample t-tests, we further tested the main effect of HRV across all subjects, as well as for each age group separately. For each statistical analysis, a positive and a negative contrast were computed. Only results surviving whole-brain family-wise error (FWE) correction at $p < 0.05$ (cluster-level) with a voxel-level threshold of $p < 0.001$ were considered significant. All (unthresholded) statistical maps are available at NeuroVault (Gorgolewski et al., 2015) for detailed inspection in 3D (http://neurovault.org/collections/TELEUIIY).

2.5.Cognitive measurement and potential confounding factors for HRV

Sex. As HRV has been reported to differ between sexes (Koenig and Thayer, 2016; Voss et al., 2015), we analyzed sex differences in HRV per age group in a 2 (sex) × 3 (age group) ANOVA.

Smoking. Since smoking has a short- and long-term impact on HRV (Felber Dietrich et al., 2007; Hayano et al., 1990), we examined potential effects of smoking status on HRV. To this end, we classified subjects into three groups (smokers: N= 75, former smokers: N=84, and non-smokers: N=220, [no info available: NA=9]). We used a 2 (sex) x 3 (smoking) ANOVA to test the mean differences between the groups using sex as additional between-subjects factor.

Cognition. The Trail Making Test (TMT) is a cognitive test measuring executive function, including processing speed and mental flexibility. By drawing lines, subjects sequentially connect numbers and/or letters while their reaction times are recorded (Reitan, 1955; Reitan and Wolfson, 1995). In the first part of the test (TMT-A) the targets are all numbers (1, 2, 3, etc.), while in the second part (TMT-B), participants need to alternate between numbers and letters (1, A, 2, B, etc.). In both TMT A and B, the time to complete the task quantifies the performance and lower scores indicate better performance.

Blood Pressure. Systolic blood pressure (SBP) and diastolic blood pressure (DBP) were

286 measured in a seated position using an automatic oscillometric blood pressure monitor (LIFE
287 sample; OMRON 705IT, LEMON sample; OMRON M500) after a resting period of 5 min.
288 While in the LIFE sample three consecutive blood pressure measurements were taken from
289 the right arm in intervals of 3 minutes, in the LEMON sample measurements were taken from
290 participants' left arms on three separate occasions within two weeks. In each sample, all
291 available measurements per participant were averaged to one systolic and one diastolic blood
292 pressure value.

293 *Anthropometric measurements.* Subjects' heights and weights were taken according to a
294 standardized protocol by trained study staff. Body mass index (BMI; in kg/m^2) was calculated
295 by dividing the body weight by the square of the body height, while waist to hip ratio (WHR)
296 was calculated as waist circumference measurement divided by hip circumference
297 measurement (Huxley et al., 2010). As a control, all analyses on the association between HRV
298 and the brain across the age groups were repeated with blood pressure (BP) and body mass
299 index (BMI) as additional covariates of no interest.

300 For cognition, blood pressure, and anthropometric measurements, we assessed age-group
301 differences statistically using one-way ANOVAs, and then tested their association with HRV
302 using Spearman correlations for each age group. To determine statistical significance, we
303 used a two-sided α-level of 0.05. Statistical analyses were conducted using R version 3.3.2 (R
304 Core Team 2016).

3. Results

Details about the demographic, anthropometric, cardiovascular, and cognitive characteristics of the 388 participants can be found in Table 1. The age groups differed significantly in all variables (Table 1).

Table 1. Participant characteristics for each age group. For continuous variables, data is provided in means and standard deviations (in parenthesis). One-way ANOVAs were used to detect age group differences.

	Young (20-35 years) (N=140)	Middle (35-60 years) (N=119)	Old (60-80 years) (N=129)	df	F-value	Eta-squared (η^2)
Age	26.01 (4.17)	46.39 (6.25)	66.88 (4.68)			
Sex	38 M /102 F	36 M / 83 F	50 M / 79 F		4.38‡	
Resting HRV (RMSSD in ms)	53 (27.11)	32.77 (21.01)	27.27 (22.99)	385	43.01***	0.182
Mean HR (1/min)	64.38 (9.62)	62.93 (10.01)	66.24 (10.44)	385	3.411*	0.017
RR interval (ms)	952.56 (137.06)	977.87 (149.75)	928.32 (148.53)	385	3.62*	0.018
mean FD (mm)	0.18 (0.05)	0.28 (0.10)	0.31 (0.11)	385	82.61***	0.300
BMI (kg/m^2)	23.58 (3.03)	26.51 (3.62)	26.54 (3.57)	382	33.34***	0.148
WHR	0.86 (0.07)	0.92 (0.08)	0.95 (0.08)	381	47.64***	0.200
SBP (mmHg)	122.08 (11.42)	126.55 (13.74)	138.76 (18.2)	381	45.45***	0.192
DBP (mmHg)	71.23 (7.33)	78.21 (9.11)	80.00 (10.44)	381	35.47***	0.156
TMT A (s)	24.95 (7.79)	30.33 (12.73)	40.01 (13.54)	384	58.48***	0.233
TMT B (s)	57.72 (17.89)	71.40 (39.04)	95.15 (45.09)	382	45.73***	0.193

312 **p < 0.05; **p < 0.01; ***p < 0.001, 2-tailed*

313 ‡ Kruskal-Wallis-Test

314 *Note.* HRV = heart rate variability; RMSSD = root mean square of successive differences; HR
315 = heart rate, FD = framewise displacement; BMI = body mass index; WHR = waist to hip
316 ratio; SBP = systolic blood pressure; DBP = diastolic blood pressure; TMT = trail making
317 test.

318

319 There was a significant main effect of age group on HRV ($F(2,382) = 63.552$, $p = 2 \times 10^{-16}$,
320 $\eta^2 = 0.182$), sex did not show a significant main effect on HRV ($F(1,382) = 0.187$, $p =$
321 0.666), and there was no significant age group × sex interaction on HRV ($F(2,382) = 0.233$, p
322 = 0.792). HRVs of smokers, former smokers, and non-smokers did not differ significantly
323 from each other (main effect smoking group: $F(2,373) = 1.241$, $p = 0.290$, main effect of sex:
324 $F(1,373) = 0.473$, $p = 0.492$; smoking group × sex interaction: $F(2,373) = 0.606$, $p = 0.546$).
325 HRV was negatively correlated with age (rho = -0.21, p = 0.010), BMI (rho = -0.207, p
326 = 0.020), and DBP (rho = -0.231, p = 0.012) within the middle-aged individuals. No
327 significant associations were found between HRV and mean FD, SBP, WHR, TMT A, and
328 TMT B in any of the age groups (Supplementary Table 1).
329 *Voxel-based Morphometry (VBM).* There was no significant association between HRV
330 and GMV across all subjects. Also, an ANOVA did not yield a significant age group x HRV
331 interaction on GMV. While an exploratory one-sample t-test in the middle-aged group
332 indicated a significant HRV-related increase of GMV in left cerebellum (MNI coordinates: [-
333 15, -87, -51], k = 1540, T = 3.92, pFWE = 0.004), there were no significant effects of HRV on
334 GMV for younger and older adults. Control analyses that included BP and BMI as covariates
335 of no interest did not change the results.

Eigenvector Centrality Mapping (ECM). A significant effect of age group on the relation between resting HRV and EC was detected in the bilateral vmPFC (MNI coordinates: [0, 57, -6], k = 62, F = 10.79). The beta values from bilateral vmPFC for each age group are plotted in Figure 1A, suggesting that younger adults show a stronger association between HRV and EC in bilateral vmPFC than middle-aged and older individuals (Table 2). This was supported by post-hoc two-sample t-tests, which indicated that the correlation between HRV and EC in bilateral vmPFC was significantly stronger for the contrasts of young > old and young > middle-age (Table 2). A one-sample t-test across all subjects showed increased EC with higher HRV in bilateral PCC (Figure 1B). The negative contrast did not yield any significant results. In separate one-sample t-tests for each age group, we found HRV-dependent EC increases in right vmPFC, bilateral PCC, and superior frontal gyrus (SFG), as well as HRV-dependent EC decreases in left superior occipital gyrus (SOG) including cuneus and calcarine sulcus in the group of young subjects. Our data did not show any significant positive or negative correlation with HRV in the groups of middle-aged and old subjects that were correctable for multiple comparisons. The complete ECM results are presented in Table 2. Control analyses that included BP and BMI as covariates of no interest did not change the results.

353 **Fig. 1.** Association between resting heart rate variability (HRV), measured as root mean square
354 of successive differences (RMSSD), and eigenvector centrality (EC). **A)** The interaction
355 between age group and HRV was significant in the bilateral ventromedial prefrontal cortex
356 (vmPFC; MNI coordinates: [0, 57, -6], k = 62, F = 10.79, pFWE = 0.006), displayed at x = -3.
357 **B)** An increased EC in the bilateral posterior cingulate cortex (PCC; MNI coordinates [6, -54,
358 36], k = 204, T = 5.29, pFWE < 0.001) across all age groups, displayed at x = 6. Results are
359 shown at a voxel threshold of p < 0.001 with family-wise error (FWE) correction with p < 0.05
360 at the cluster level.

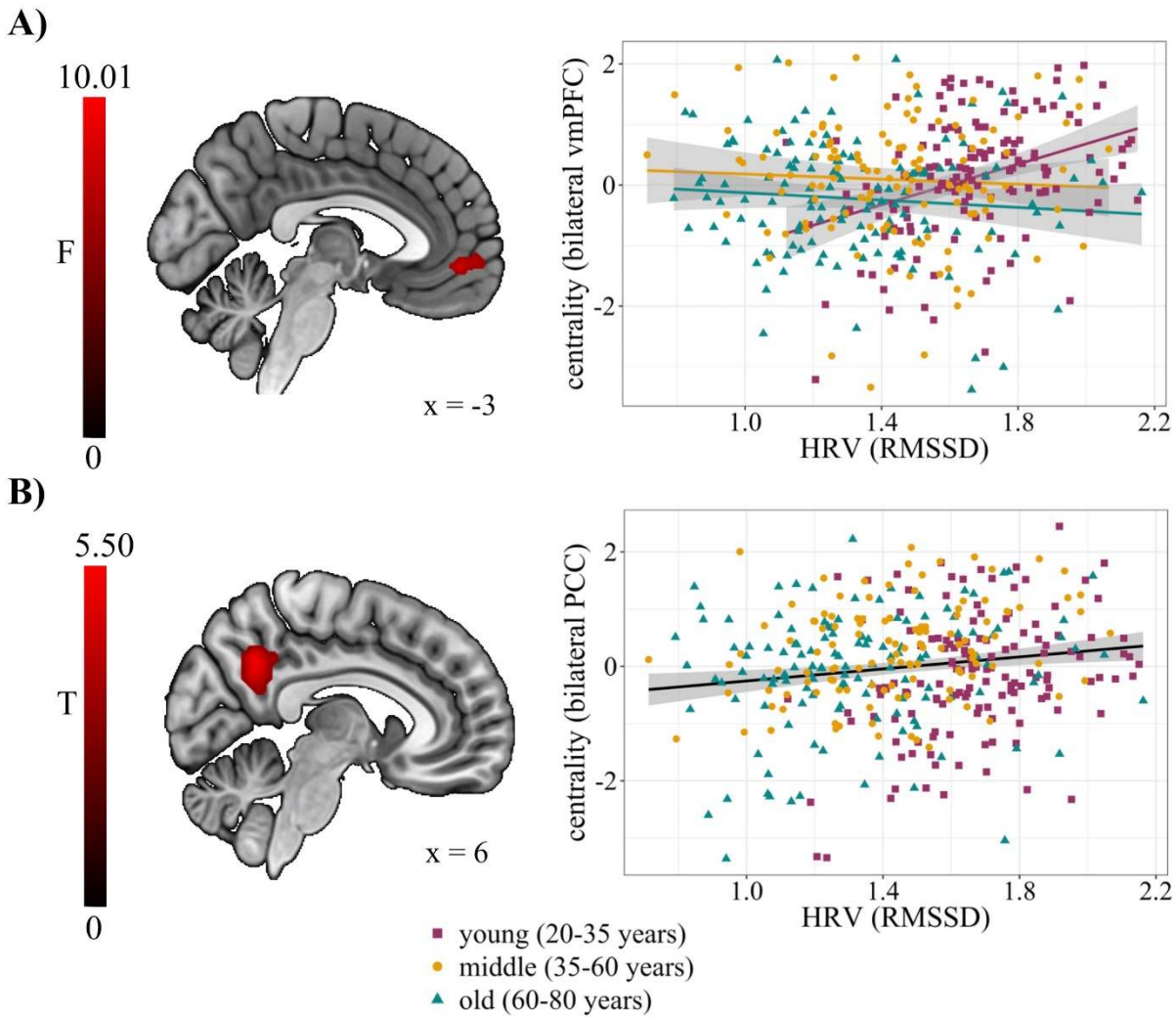

361

362 **Table 2.** Brain regions that show significant increases or decreases in eigenvector centrality
363 with heart rate variability (HRV). Thresholds: $p < 0.001$ at the voxel and $p < 0.05$ with
364 family-wise error (FWE) correction at the cluster level.

	Regions	H	cluster size k (Voxel)	MNI coordinates			FWE	z	F/T-value
				x	y	z			
ANOVA	Ventromedial prefrontal cortex	R/L	62	0	57	-6	0.006	4.03	10.79
				-3	48	-6		3.76	9.63
				0	60	3		3.49	8.53
Across age groups (+)	Posterior cingulate cortex /precuneus	R/L	204	6	-54	36	<0.001	5.29	5.39
				-9	-57	33		4.04	4.09
				-12	-51	45		3.35	3.38
Young (+)	Ventromedial prefrontal cortex	R	316	0	57	-6	<0.001	5.07	5.16
				6	51	9		4.89	4.98
				15	60	15		4.22	4.16
	Posterior cingulate cortex /precuneus	R/L	167	6	-57	27	<0.001	4.46	4.52
				-9	-54	18		3.72	3.75
				-9	-60	27		3.70	3.74
	Superior frontal gyrus	R/L	240	15	33	48	0.002	4.50	4.56
				15	48	39		4.32	4.37
				-6	36	48		4.24	4.29
Young (-)	Superior occipital gyrus	L	129	-6	-96	3	<0.001	4.63	4.70
				-15	-99	-3		4.24	4.29
				0	-84	-3		3.71	3.76
Middle (+)	n.s								
Middle (-)	n.s								
Old (+)	n.s								
Old (-)	n.s								
Young > Old	Ventromedial prefrontal cortex	R	131	0	57	-6	<0.001	4.45	4.51
				0	60	3		4.01	4.05
				-3	45	-8		3.62	3.65
Young < Old	n.s								
Middle > Young	n.s								
Middle < Young	Ventromedial prefrontal cortex	R	85	3	45	-6	0.005	4.09	4.13
				-12	48	-9		4.06	4.11
				6	45	15		3.58	3.61
Old > Middle	n.s								
Old < Middle	n.s								

365 *Note.* R= right, L = left, H = hemisphere, ANOVA = analysis of variance, MNI = Montreal
366 Neurological Institute, n.s = not significant
367
368 *Exploratory Seed-based Functional Connectivity Analysis (SBCA).* In the additional
369 exploratory seed-based functional connectivity analysis, a significant effect of age group on
370 the relation between resting HRV and whole-brain bilateral vmPFC connectivity was found in
371 bilateral cerebellum, right superior parietal lobe (SPL), left middle occipital gyrus (MOG) and
372 inferior occipital gyrus (IOG), and left SFG extended to supplementary motor area (SMA).
373 The beta values from the right cerebellum for each age group are plotted in Figure 2A,
374 suggesting that younger adults show stronger functional connectivity between bilateral
375 vmPFC and right cerebellum than middle-aged and older individuals (Table 3). The post-hoc
376 two-sample t-tests similarly indicated that higher HRV levels were significantly correlated
377 with stronger functional connectivity between bilateral vmPFC and bilateral cerebellum, right
378 SPL, left MOG, left post-central gyrus, and left SMA for the contrasts of young > old and
379 young > middle (Table 3). A one-sample t-test in the overall sample, to assess the association
380 between HRV and bilateral vmPFC connectivity, showed an increased functional connectivity
381 with left middle frontal gyrus (MFG) extending to dorsolateral prefrontal cortex (DLPFC)
382 (Figure 2B). Separate one-sample t-tests for each age group showed no significant association
383 for the middle-aged and old subjects but an increased vmPFC connectivity in distributed brain
384 regions including bilateral cerebellum, bilateral MOG, and right SMA for the young subjects.
385 We did not observe any significant negative correlations neither in the overall sample nor in
386 each age group. Control analyses that included BP and BMI as covariates of no interest did
387 not change the results. The complete SBCA results are presented in Table 3.
388

389 **Fig. 2.** Association between resting heart rate variability (HRV), measured as root mean square
390 of successive differences (RMSSD), and brain function in an exploratory seed-based functional
391 connectivity analysis originating from bilateral ventromedial prefrontal cortex (vmPFC). **A)**
392 The interaction between age group and HRV was significant in the right cerebellum (MNI
393 coordinates [33, -42, -45], k = 46, F = 15.19, pFWE < 0.001), displayed at x = 33. **B)** An
394 increased functional connectivity in the right dorsolateral prefrontal cortex (DLPFC; MNI
395 coordinates [-30, 54, 12], k = 67, T = 4.10, pFWE = 0.032) was found across all age groups,
396 displayed at z = 12. Results are shown at a voxel threshold of p < 0.001 with family-wise error
397 (FWE) correction with p < 0.05 at the cluster level.

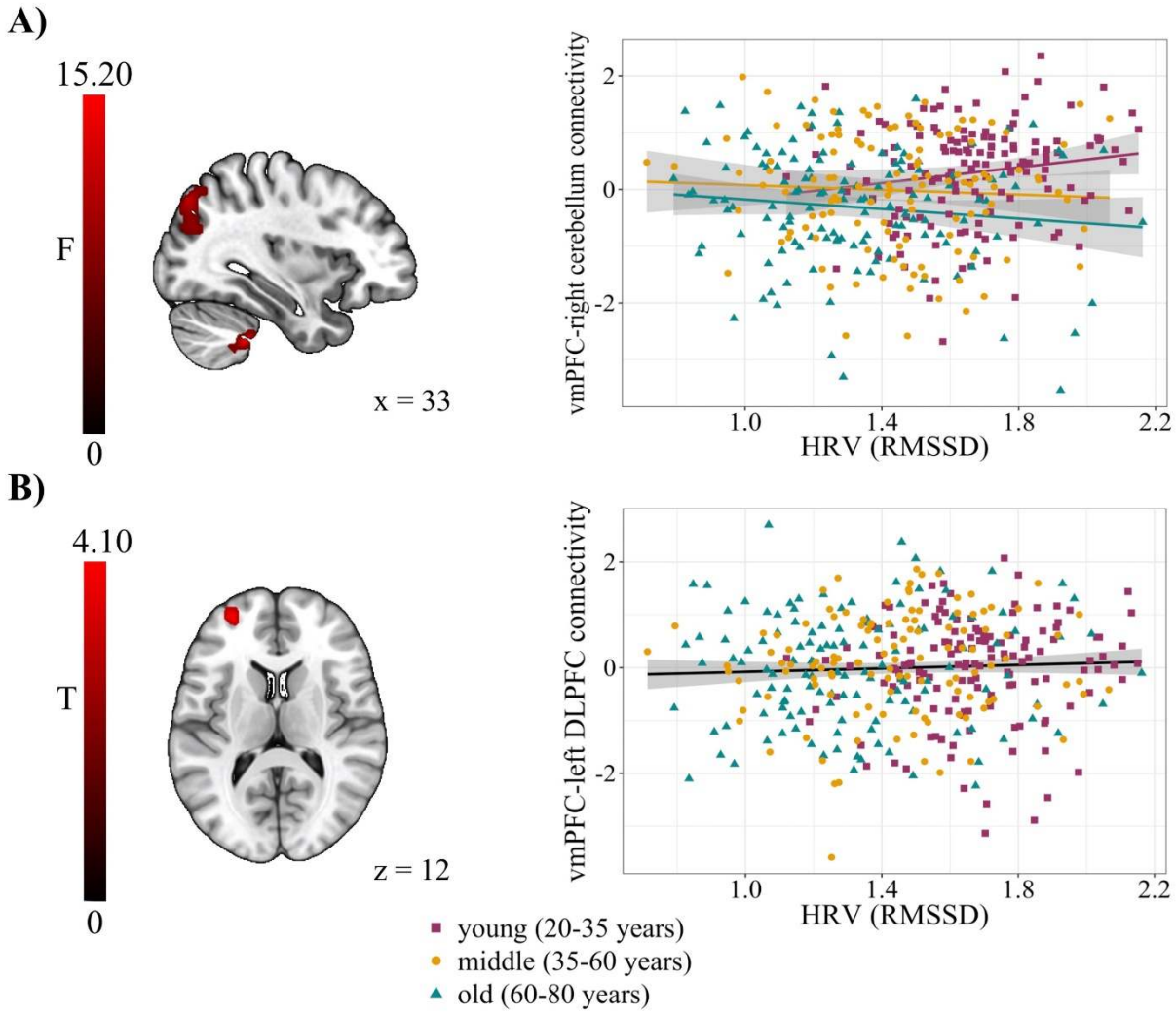

398

399 **Table 3.** Brain regions that show resting heart rate variability-related connectivity with the
400 bilateral ventromedial prefrontal cortex (vmPFC) in an exploratory seed-based functional
401 connectivity analysis. Thresholds: $p < 0.001$ at the voxel and $p < 0.05$ with family-wise error
402 (FWE) correction at the cluster level.

	Regions	H	cluster size k (Voxels)	MNI coordinates			FWE	z	F/T-value
				x	y	z			
ANOVA	Cerebellum	R	46	33	-42	-45	0.049	4.91	15.19
	Superior parietal lobe	R	203	24	-75	51	<0.001	4.48	12.94
				33	-78	45		4.34	12.25
				36	-75	30		3.82	9.88
	Middle occipital gyrus	L	57	-33	-84	30	0.021	4.24	11.74
				-39	-66	24		3.31	7.84
	Inferior occipital gyrus		60	-33	-69	-6	0.016	3.85	9.97
				-42	-63	-3		3.76	9.61
				-51	-69	-15		3.62	9.03
	Cerebellum	L	61	-30	-60	-30	0.015	3.83	9.91
				-33	-66	-21		3.59	8.91
				-39	-72	-18		3.58	8.87
	Superior frontal gyrus extended to supplementary motor area	L	71	0	15	66	0.007	3.73	9.47
				0	3	57		3.6	8.96
				9	12	57		3.53	8.66
Across age groups (+)	Middle frontal gyrus extended to dorsolateral prefrontal cortex	L	67	-30	54	12	0.032	4.06	4.10
				-36	54	3		3.54	3.57
				-18	51	3		3.39	3.42
Young (+)	Cerebellum	R	131	33	-42	-45	0.001	5.06	5.15
				42	-60	-48		4.68	4.75
				36	-63	-39		3.29	3.31

	Cerebellum	L	116	-12	-57	-54	0.002	4.6	4.67
				-21	-69	-54		4.2	4.25
				-15	-48	-51		4.09	4.14
	Middle occipital gyrus	R	163	39	-75	42	<0.001	4.46	4.52
				30	-69	51		4.15	4.20
				21	-78	51		3.63	3.67
	Middle occipital gyrus	L	131	-39	-66	24	0.001	4.31	4.37
				-33	-84	30		3.94	3.98
				-39	-60	12		3.47	3.50
	Cerebellum	R	63	18	-75	-18	0.04	4.13	4.18
				27	-81	-18		3.68	3.72
				18	-84	-15		3.64	3.67
	Cerebellum	L	102	-33	-81	-21	0.005	4.13	4.18
				-30	-60	-30		3.7	3.74
				-21	-90	-15		3.59	3.62
	Supplementary motor area	R	87	3	6	54	0.01	3.77	3.81
				0	15	69		3.68	3.72
				9	12	57		3.59	3.63
Young (-)	n.s								
Middle (+)	n.s								
Middle (-)	n.s								
Old (+)	n.s								
Old (-)	n.s								
Young > Old	Cerebellum	R	67	33	-42	-45	0.032	4.59	4.66
				15	-48	-51		3.63	3.67
				27	-57	-45		3.41	3.44
	Inferior occipital gyrus	L	237	-33	-69	-6	<0.001	4.41	4.47
				-42	-63	-3		4.33	4.38
				-39	-72	-18		4.14	4.19

	Superior parietal lobe	R	275	24	-78	51	<0.001	4.31	4.37
				36	-75	45		4.21	4.26
				36	-75	27		3.95	4
	Middle occipital gyrus	L	140	-27	-84	27	0.001	4.30	4.35
				-36	-66	24		3.89	3.93
				-39	-60	12		3.62	3.65
	Superior frontal gyrus extended to supplementary motor area	L	147	-3	3	57	0.001	3.99	4.04
				12	6	63		3.72	3.75
				3	12	66		3.61	3.65
	Postcentral gyrus	R	72	42	-6	30	0.024	3.87	3.91
				54	6	24		3.69	3.73
				54	0	33		3.53	3.56
	Superior frontal gyrus extended to supplementary motor area	R	73	3	-18	60	0.022	3.62	3.66
				-3	-36	69		3.56	3.59
				3	-9	69		3.29	3.31
Young < Old	n.s								
Middle > Young	n.s								
Middle < Young	Cerebellum	R	189	33	-42	-45	<0.001	4.99	5.08
				42	-60	-48		4.60	4.67
				18	-45	-51		4.34	4.40
	Superior parietal lobe	R	270	27	-72	51	<0.001	4.76	4.83
				33	-78	45		4.51	4.58
				36	-75	30		4.04	4.09
	Cerebellum	L	239	-12	-57	-54	<0.001	4.74	4.82
				-15	-45	-51		4.61	4.68
				-12	-39	-45		4.36	4.42
	Middle occipital gyrus	L	76	-33	-84	30	0.019	4.59	4.66
				-45	-72	27		3.37	3.40

	Cerebellum	L	313	-30	-60	-30	<0.001	4.27	4.32
				12	-69	-21		4.18	4.23
				18	-78	-18		3.95	3.99
	Superior frontal gyrus extended to supplementary motor Area	L	109	0	15	66	0.003	4.19	4.24
				15	9	69		3.61	3.64
Old > Middle	n.s								
Old < Middle	n.s								

Note. R= right, L = left, H = hemisphere, ANOVA = analysis of variance, MNI = Montreal Neurological Institute

405 # 4. Discussion

406 In the present study, we assessed the relationship between parasympathetic
407 cardioregulation (using resting HRV) and brain structure (using VBM) as well as whole-brain
408 resting-state connectivity (using ECM and SBCA) in a large sample of healthy young,
409 middle-aged, and old participants. We found the frequently observed age-related decrease in
410 resting HRV (Almeida-Santos et al., 2016; Voss et al., 2015) to be accompanied by alterations
411 in brain function. Specifically, higher HRV was linked to stronger network centrality in
412 several brain regions, particularly along the cortical midline. In the PCC, this correlation was
413 present in all age groups while in the vmPFC, network centrality was related to higher HRV
414 in young but not in middle-aged and old adults. These findings support the view that altered
415 HRV during aging may have a functional brain component associated with it.

416 ## 4.1.Age-dependent association of resting HRV with functional connectivity

417 Given the relationship between HRV and age (Almeida-Santos et al., 2016; Voss et
418 al., 2015), HRV and brain structure (Wei et al., 2018), as well as HRV and brain function
419 (Sakaki et al., 2016), we hypothesized the neural correlates of resting HRV to be also age-
420 dependent. Our results confirm that the relationship between HRV and network centrality at
421 rest differs between age groups. Evidence is accumulating that alterations of intrinsic brain
422 activity are a key feature of normal brain aging (Damoiseaux et al., 2008): age-dependent
423 intrinsic connectivity alterations in the DMN have been found not only in healthy aging
424 (Ferreira and Busatto, 2013) but also in (age-related) pathologies, for example, in individuals
425 with a high familial risk for depression (Posner et al., 2016) and in young APOE-ε4 carriers
426 (Filippini et al., 2009), which is a possible biomarker for Alzheimer's dementia (Kanekiyo et
427 al., 2014). Our results that resting HRV is related to increased network centrality in medial
428 frontal regions in the young but not in the middle-aged and old age group could be interpreted
429 in the framework of the functional plasticity hypothesis of cognitive aging (Greenwood,

2007). According to this hypothesis, the structural vulnerability particularly of prefrontal cortex leads to an age-related functional reorganization (e.g., Grady, 2012; for a detailed review). Changes in the resting-state network architecture around the vmPFC that are related to parasympathetic cardioregulation could thus represent altered cardiovascular control with advancing age and concomitant network reorganization.

In addition to the age-dependent association of resting HRV with functional brain network centrality in medial frontal regions, we also found an HRV-related bilateral medial parietal cluster in the PCC that was independent of age. Both vmPFC and PCC are central nodes of the DMN (Greicius et al., 2003; Uddin et al., 2009) and have been related to self-generated or internally directed mental processes like thoughts and feelings (Andrews-Hanna et al., 2014; Raichle et al., 2001). Regions of the DMN – and particularly its medial frontal (e.g., vmPFC) and parietal components (e.g., PCC and precuneus) – have also been implied in the central processing of autonomic – and particularly parasympathetic – function (Beissner et al., 2013; Benarroch, 1993). It is plausible that in the absence of external stimulation, brain function (i.e., activity and connectivity) is predominantly allocated to the "internal milieu", that is, to monitoring and regulating bodily signals (e.g., the parasympathetic "rest-and-digest"). Fittingly, the PCC has been found active in tasks that involved the assessment of self-relevance (Yu et al., 2011) as well as self-location and body ownership (Guterstam et al., 2015), while the vmPFC was related to processing bodily information (Gusnard et al., 2001), autonomic control (Critchley et al., 2011), and cardiovascular arousal (Wong et al., 2007). Similarly, a causal role of the PFC for cardiovascular activity (e.g., HR and HRV) was found in a meta-analysis of non-invasive brain stimulation and autonomic functioning (Makovac et al., 2017).

The exploratory SBCA similarly showed an age-dependent relationship between resting HRV and functional brain connectivity. Specifically, we found stronger functional

455 connectivity between bilateral vmPFC and a widespread set of brain regions including
456 bilateral cerebellum, occipital gyrus, right SPL, and SFG extending to SMA in young but not
457 middle-aged and old adults. These results extend the ECM findings by suggesting additional
458 cortico-cerebellar regions might be involved in the modulation of visceral processes. In line
459 with this interpretation, activation in the cerebellum has been connected to the regulation of
460 visceral responses (Demirtas-Tatlidede et al., 2011), fear conditioning (Leaton, 2003;
461 Sacchetti et al., 2002), feeding (Tataranni et al., 1999), as well as the coordination and control
462 of cardiovascular activities (Bradley et al., 1991; Ghelarducci and Sebastiani, 1996).
463 Furthermore, autonomic activity during cognitive and motor tasks was positively associated
464 with activation in the cerebellum and, among other regions, the SMA and dorsal ACC
465 (Critchley et al., 2003).

466 Despite previous evidence of the relationship between brain structure and vagally-
467 mediated HRV in central autonomic network regions (Wei et al., 2018), using whole-brain
468 VBM analysis, we only found a significant GMV change related with resting HRV in the
469 cerebellum for the middle-aged group. Notably, in the study by Wei et al. (2018) reduced GM
470 volume in the cerebellum was associated with HR (but not HRV) in healthy middle-aged
471 individuals. The divergent results could be due to different measurement parameters (e.g.,
472 MRI sequence parameters) but also to different effect size and statistical power (for more
473 details see *Limitations*).

474 4.2.Physiological and psychophysiological interpretations of HRV

475 The most fundamental (purely physiological) understanding of the role of the ANS –
476 and particularly the PNS – is to ensure visceral and cardiovascular functioning or bodily
477 homeostasis – by allowing rapid adaptive behavioral and physiological reactions in ever-
478 changing environments or by disengagement and relaxation in resting moments ("rest-and-
479 digest"; e.g., Cannon, 1929).

More *psycho*physiological interpretations of ANS function have extended this view to cognitive, affective, and social phenomena: For example, the two main theoretical perspectives of HRV – the polyvagal theory (Porges, 2007, 2001, 1995) and the neurovisceral integration model (Smith et al., 2017; Thayer and Lane, 2000; Thayer and Ruiz-Padial, 2006) – suggest that PNS activation can serve as a biomarker of what can be summarized as "top-down" self-regulation (Holzman and Bridgett, 2017). The polyvagal theory (Porges, 2007) takes an evolutionary approach, according to which the role of the ANS and particularly the vagus nerve can be understood as increasing adaptability through socially engaged behaviors (e.g., self-soothing) and inhibition of sympathetic-adrenal influences on the body (Porges, 2007). The neurovisceral integration model (Smith et al., 2017; Thayer and Lane, 2000; Thayer and Ruiz-Padial, 2006) highlights the role of vagally-mediated HRV for emotional or self-regulation. This model explicitly links the brain and the rest of the body by assuming that the PFC – and particularly the vmPFC – tonically inhibits the amygdala, which affects autonomic function, thereby linking both nervous systems to inhibitory or (self-)regulatory processes (Kemp et al., 2017; Thayer et al., 2012). Convergently, resting HRV has recently been associated with vmPFC activation during a dietary self-control task in young adults (Maier and Hare, 2017). Both theories draw on evidence that higher HRV is indicative of better bodily functioning by enabling physiological and behavioral adaptation through cognitive and socio-emotional flexibility. Taken together, our findings are consistent with both the polyvagal theory and the neurovisceral integration model of HRV and extend them by providing evidence for a brain network component of vagally-mediated HRV in healthy aging.

5. Limitations

There are a number of limitations that should be considered in the interpretation of our results. The study design is cross-sectional and does not allow us to infer the directionality of the association between resting HRV and the brain. Additionally, our health criteria also allowed inclusion of subjects with higher BMI (>25 kg/m^2) or untreated/undiagnosed hypertension (SBP > 140 mmHg, DBP > 90 mmHg). This makes it difficult to disentangle HRV-related influences from other bodily/cardiovascular influences – which are also physiologically related (BMI: Molfino et al., 2009; BP: Singh et al., 1998). However, control analyses that accounted for BP and BMI showed very similar results of the association between resting HRV and the brain. Although psychological interpretations of a single physiological marker like resting HRV are intrinsically limited, previous studies have associated HRV with different trait or state levels of, for example, executive control (Capuana et al., 2014), stress (Sin et al., 2016), and emotion regulation (Williams et al., 2015). For a psychological interpretation of our finding that the association between HRV and functional connectivity at rest is age-dependent, similar analyses on task-related parasympathetic and neural activity could be helpful. Although we accounted for systematic study differences in the second-level GLM, different acquisition parameters of the rs-f/MRI and ECG may have influenced our results (e.g., for structural MRI; Streitbürger et al., 2014). Further, we calculated the RMSSD using 10 s of ECG data, which has been shown to be a valid measurement (Munoz et al., 2015; Nussinovitch et al., 2011a, 2011b). Nevertheless, ECG data recorded over longer periods (e.g., 24-hour) can complement this “ultra-short” evaluation of parasympathetic function.

6. Conclusion

In this cross-sectional study, we examined the association of resting HRV with brain structure and functional brain connectivity in different age groups of healthy adults. Our main findings are correlations between resting HRV and brain network architecture in the PCC across all age groups and in the vmPFC in young but not in middle-aged and old subjects. These support the view that the well-known HRV decrease with age may have a functional brain network component along the cortical midline. Consistent with the role of these areas in affective, cognitive, and autonomic regulation, our results provide a comprehensive picture of the differential effect of age on heart-brain interactions and extend our knowledge of parasympathetic cardioregulation being important for healthy aging.

7. Financial disclosures

The authors declare no conflict of interest

8. Acknowledgments

This study was supported by LIFE Leipzig Research Center for Civilization Diseases at the University of Leipzig funded by the European Union, European Regional Development Fund, and the Free State of Saxony. The authors would like to thank all volunteers for their participation in one of the two studies. Further, we thank all researchers, technicians and students who planned, collected, entered and curated data, used in this manuscript.

9. References

Almeida-Santos, M.A., Barreto-Filho, J.A., Oliveira, J.L.M., Reis, F.P., da Cunha Oliveira, C.C., Sousa, A.C.S., 2016. Aging, heart rate variability and patterns of autonomic regulation of the heart. Arch. Gerontol. Geriatr. 63, 1–8. doi:10.1016/j.archger.2015.11.011

Andrews-Hanna, J.R., Smallwood, J., Spreng, R.N., 2014. The default network and self-generated thought: Component processes, dynamic control, and clinical relevance. Ann. N. Y. Acad. Sci. 1316, 29–52. doi:10.1111/nyas.12360

Arking, R., 2006. The biology of aging: observations and principles, The Biology of Aging Observations Principles. doi:10.1080/03601270701498491

Ashburner, J., 2007. A fast diffeomorphic image registration algorithm. Neuroimage 38, 95–113. doi:10.1016/j.neuroimage.2007.07.007

Ashburner, J., Friston, K.J., 2000. Voxel-Based Morphometry—The Methods. Neuroimage 11, 805–821. doi:10.1006/nimg.2000.0582

Avants, B.B., Tustison, N.J., Song, G., Cook, P.A., Klein, A., Gee, J.C., 2011. A reproducible evaluation of ANTs similarity metric performance in brain image registration. Neuroimage 54, 2033–2044. doi:10.1016/j.neuroimage.2010.09.025

Babayan, A., Erbey, M., Kumral, D., Reinelt, R. D., Reiter, A. M. F., Röbbig, J., Schaare, L. H., Uhlig, M., … Gaebler, M., Villringer, A., A Mind-Brain-Body dataset of MRI, EEG, cognition, emotion, and peripheral physiology in young and old adults, under review.

Bazin, P.L., Weiss, M., Dinse, J., Schäfer, A., Trampel, R., Turner, R., 2014. A computational framework for ultra-high resolution cortical segmentation at 7 Tesla. Neuroimage 93, 201–209. doi:10.1016/j.neuroimage.2013.03.077

Behzadi, Y., Restom, K., Liau, J., Liu, T.T., 2007. A component based noise correction

569 method (CompCor) for BOLD and perfusion based fMRI. Neuroimage 37, 90–101.
570 doi:10.1016/j.neuroimage.2007.04.042
571 Beissner, F., Meissner, K., Bar, K.-J., Napadow, V., 2013. The Autonomic Brain: An
572 Activation Likelihood Estimation Meta-Analysis for Central Processing of Autonomic
573 Function. J. Neurosci. 33, 10503–10511. doi:10.1523/JNEUROSCI.1103-13.2013
574 Benarroch, E.E., 1993. The Central Autonomic Network: Functional Organization,
575 Dysfunction, and Perspective. Mayo Clin. Proc. 68, 988–1001. doi:10.1016/S0025-
576 6196(12)62272-1
577 Bradley, D.J., Ghelarducci, B., Spyer, K.M., 1991. The role of the posterior cerebellar vermis
578 in cardiovascular control. Neurosci. Res. 12, 45–56. doi:10.1016/0168-0102(91)90099-K
579 Buccelletti, E., Gilardi, E., Scaini, E., Galiuto, L., Persiani, R., Biondi, a, Basile, F., Silveri,
580 N.G., 2009. Heart rate variability and myocardial infarction: systematic literature review
581 and metanalysis. Eur. Rev. Med. Pharmacol. Sci. 13, 299–307.
582 Cannon, W.B., 1929. Organization for Physiological Homeostasis. Physiol. Rev. 9, 399–431.
583 doi:10.1152/physrev.1929.9.3.399
584 Capuana, L.J., Dywan, J., Tays, W.J., Elmers, J.L., Witherspoon, R., Segalowitz, S.J., 2014.
585 Factors influencing the role of cardiac autonomic regulation in the service of cognitive
586 control. Biol. Psychol. 102, 88–97. doi:10.1016/j.biopsycho.2014.07.015
587 Chang, C., Metzger, C.D., Glover, G.H., Duyn, J.H., Heinze, H.J., Walter, M., 2013.
588 Association between heart rate variability and fluctuations in resting-state functional
589 connectivity. Neuroimage 68, 93–104. doi:10.1016/j.neuroimage.2012.11.038
590 Cox, R.W., 1996. AFNI: Software for Analysis and Visualization of Functional Magnetic
591 Resonance Neuroimages. Comput. Biomed. Res. 29, 162–173.
592 doi:10.1006/cbmr.1996.0014
593 Critchley, H.D., Corfield, D.R., Chandler, M.P., Mathias, C.J., Dolan, R.J., 2000. Cerebral

correlates of autonomic cardiovascular arousal: a functional neuroimaging investigation in humans. J. Physiol. 523 Pt 1, 259–270. doi:10.1111/j.1469-7793.2000.t01-1-00259.x

Critchley, H.D., Mathias, C.J., Josephs, O., O'Doherty, J., Zanini, S., Dewar, B.K., Cipolotti, L., Shallice, T., Dolan, R.J., 2003. Human cingulate cortex and autonomic control: Converging neuroimaging and clinical evidence. Brain 126, 2139–2152. doi:10.1093/brain/awg216

Critchley, H.D., Nagai, Y., Gray, M.A., Mathias, C.J., 2011. Dissecting axes of autonomic control in humans: Insights from neuroimaging. Auton. Neurosci. Basic Clin. 161, 34–42. doi:10.1016/j.autneu.2010.09.005

Damoiseaux, J.S., Beckmann, C.F., Arigita, E.J.S., Barkhof, F., Scheltens, P., Stam, C.J., Smith, S.M., Rombouts, S.A.R.B., 2008. Reduced resting-state brain activity in the "default network" in normal aging. Cereb. Cortex 18, 1856–1864. doi:10.1093/cercor/bhm207

De Meersman, R.E., Stein, P.K., 2007. Vagal modulation and aging. Biol. Psychol. 74, 165–173. doi:10.1016/j.biopsycho.2006.04.008

Demirtas-Tatlidede, A., Freitas, C., Pascual-Leone, A., Schmahmann, J.D., 2011. Modulatory effects of theta burst stimulation on cerebellar nonsomatic functions. Cerebellum 10, 495–503. doi:10.1007/s12311-010-0230-5

Felber Dietrich, D., Schwartz, J., Schindler, C., Gaspoz, J.-M., Barthélémy, J.-C., Tschopp, J.-M., Roche, F., von Eckardstein, A., Brändli, O., Leuenberger, P., Gold, D.R., Ackermann-Liebrich, U., 2007. Effects of passive smoking on heart rate variability, heart rate and blood pressure: an observational study. Int. J. Epidemiol. 36, 834–840. doi:10.1093/ije/dym031

Ferreira, L.K., Busatto, G.F., 2013. Resting-state functional connectivity in normal brain aging. Neurosci. Biobehav. Rev. 37, 384–400. doi:10.1016/j.neubiorev.2013.01.017

619 Filippini, N., MacIntosh, B.J., Hough, M.G., Goodwin, G.M., Frisoni, G.B., Smith, S.M.,
620 Matthews, P.M., Beckmann, C.F., Mackay, C.E., 2009. Distinct patterns of brain activity
621 in young carriers of the APOE- 4 allele. Proc. Natl. Acad. Sci. 106, 7209–7214.
622 doi:10.1073/pnas.0811879106
623 Fischl, B., 2012. FreeSurfer. Neuroimage 62, 774–781.
624 doi:10.1016/j.neuroimage.2012.01.021
625 Friston, K.J., Williams, S., Howard, R., Frackowiak, R.S.J., Turner, R., 1996. Movement-
626 related effects in fMRI time-series. Magn. Reson. Med. 35, 346–355.
627 doi:10.1002/mrm.1910350312
628 Ghelarducci, B., Sebastiani, L., 1996. Contribution of the cerebellar vermis to cardiovascular
629 control. J. Auton. Nerv. Syst. 56, 149–156. doi:10.1016/0165-1838(95)00068-2
630 Gianaros, P.J., Van Der Veen, F., Jennings, J.R., 2004. Regional cerebral blood flow
631 correlates with heart period and high-frequency heart period variability during working-
632 memory task: Implications for the cortical and subcortical regulation of cardiac
633 autonomic activity. Psychophysiology 41, 521–530. doi:10.1111/j.1469-
634 8986.2004.00179.x
635 Gorgolewski, K., Burns, C.D., Madison, C., Clark, D., Halchenko, Y.O., Waskom, M.L.,
636 Ghosh, S.S., 2011. Nipype: A Flexible, Lightweight and Extensible Neuroimaging Data
637 Processing Framework in Python. Front. Neuroinform. 5, 13.
638 doi:10.3389/fninf.2011.00013
639 Gorgolewski, K.J., Varoquaux, G., Rivera, G., Schwarz, Y., Ghosh, S.S., Maumet, C., Sochat,
640 V. V., Nichols, T.E., Poldrack, R.A., Poline, J.-B., Yarkoni, T., Margulies, D.S., 2015.
641 NeuroVault.org: a web-based repository for collecting and sharing unthresholded
642 statistical maps of the human brain. Front. Neuroinform. 9.
643 doi:10.3389/fninf.2015.00008

644 Grady, C., 2012. The cognitive neuroscience of ageing. Nat. Rev. Neurosci. 13, 491–505.
645 doi:10.1038/nrn3256
646 Greenwood, P.M., 2007. Functional Plasticity in Cognitive Aging: Review and Hypothesis.
647 Neuropsychology 21, 657–673. doi:10.1037/0894-4105.21.6.657
648 Greicius, M.D., Krasnow, B., Reiss, A.L., Menon, V., 2003. Functional connectivity in the
649 resting brain: A network analysis of the default mode hypothesis. Proc. Natl. Acad. Sci.
650 100, 253–258. doi:10.1073/pnas.0135058100
651 Griswold, M.A., Jakob, P.M., Heidemann, R.M., Nittka, M., Jellus, V., Wang, J., Kiefer, B.,
652 Haase, A., 2002. Generalized Autocalibrating Partially Parallel Acquisitions (GRAPPA).
653 Magn. Reson. Med. 47, 1202–1210. doi:10.1002/mrm.10171
654 Gusnard, D.A., Akbudak, E., Shulman, G.L., Raichle, M.E., 2001. Medial prefrontal cortex
655 and self-referential mental activity: Relation to a default mode of brain function. Proc.
656 Natl. Acad. Sci. 98, 4259–4264. doi:10.1073/pnas.071043098
657 Guterstam, A., Björnsdotter, M., Gentile, G., Ehrsson, H.H., 2015. Posterior cingulate cortex
658 integrates the senses of self-location and body ownership. Curr. Biol. 25, 1416–1425.
659 doi:10.1016/j.cub.2015.03.059
660 Hayano, J., Yamada, M., Sakakibara, Y., Fujinami, T., Yokoyama, K., Watanabe, Y., Takata,
661 K., 1990. Short- and long-term effects of cigarette smoking on heart rate variability. Am.
662 J. Cardiol. 65, 84–88. doi:10.1016/0002-9149(90)90030-5
663 Holzman, J.B., Bridgett, D.J., 2017. Heart rate variability indices as bio-markers of top-down
664 self-regulatory mechanisms: A meta-analytic review. Neurosci. Biobehav. Rev. 74, 233–
665 255. doi:10.1016/j.neubiorev.2016.12.032
666 Huxley, R., Mendis, S., Zheleznyakov, E., Reddy, S., Chan, J., 2010. Body mass index, waist
667 circumference and waist:hip ratio as predictors of cardiovascular riska review of the
668 literature. Eur. J. Clin. Nutr. 64, 16–22. doi:10.1038/ejcn.2009.68

669 Jenkinson, M., Beckmann, C.F., Behrens, T.E.J., Woolrich, M.W., Smith, S.M., 2012. Fsl.
670 Neuroimage 62, 782–790. doi:10.1016/j.neuroimage.2011.09.015
671 Jennings, J.R., Sheu, L.K., Kuan, D.C.H., Manuck, S.B., Gianaros, P.J., 2016. Resting state
672 connectivity of the medial prefrontal cortex covaries with individual differences in high-
673 frequency heart rate variability. Psychophysiology 53, 444–454. doi:10.1111/psyp.12586
674 Kanekiyo, T., Xu, H., Bu, G., 2014. ApoE and Aβ in Alzheimer's disease: Accidental
675 encounters or partners? Neuron. doi:10.1016/j.neuron.2014.01.045
676 Kemp, A.H., Koenig, J., Thayer, J.F., 2017. From Psychological Moments to Mortality: A
677 Multidisciplinary Synthesis on Heart Rate Variability Spanning the Continuum of Time.
678 Neurosci. Biobehav. Rev. doi:10.1016/j.neubiorev.2017.09.006
679 Kemp, A.H., Quintana, D.S., 2013. The relationship between mental and physical health:
680 Insights from the study of heart rate variability. Int. J. Psychophysiol. 89, 288–296.
681 doi:10.1016/j.ijpsycho.2013.06.018
682 Kim, D.H., Lipsitz, L.A., Ferrucci, L., Varadhan, R., Guralnik, J.M., Carlson, M.C., Fleisher,
683 L.A., Fried, L.P., Chaves, P.H.M., 2006. Association between reduced heart rate
684 variability and cognitive impairment in older disabled women in the community:
685 Women's Health and Aging Study I. J. Am. Geriatr. Soc. 54, 1751–1757.
686 doi:10.1111/j.1532-5415.2006.00940.x
687 Koenig, J., Thayer, J.F., 2016. Sex differences in healthy human heart rate variability: A
688 meta-analysis. Neurosci. Biobehav. Rev. 64, 288–310.
689 doi:10.1016/j.neubiorev.2016.03.007
690 Leaton, R., 2003. Fear and the cerebellum. Mol. Psychiatry 8, 461–462.
691 doi:10.1038/sj.mp.4001286
692 Liao, D., Cai, J., Rosamond, W., Barnes, R., Hutchinson, R., Whitsel, E., Rautaharju, P.,
693 Heiss, G., 1997. Cardiac Autonomic Function and Incident Coronary Heart Disease: A

694 Population-based Case-Cohort Study The ARIC Study. Am. J. … 145, 696–706.
695 doi:10.1093/aje/145.8.696
696 Lipsitz, L.A., Goldberger, A.L., 1992. Loss of 'Complexity' and Aging: Potential
697 Applications of Fractals and Chaos Theory to Senescence. JAMA J. Am. Med. Assoc.
698 267, 1806–1809. doi:10.1001/jama.1992.03480130122036
699 Loeffler, M., Engel, C., Ahnert, P., Alfermann, D., Arelin, K., Baber, R., Beutner, F., Binder,
700 H., Brähler, E., Burkhardt, R., Ceglarek, U., Enzenbach, C., Fuchs, M., Glaesmer, H.,
701 Girlich, F., Hagendorff, A., Häntzsch, M., Hegerl, U., Henger, S., Hensch, T., Hinz, A.,
702 Holzendorf, V., Husser, D., Kersting, A., Kiel, A., Kirsten, T., Kratzsch, J., Krohn, K.,
703 Luck, T., Melzer, S., Netto, J., Nüchter, M., Raschpichler, M., Rauscher, F.G., Riedel-
704 Heller, S.G., Sander, C., Scholz, M., Schönknecht, P., Schroeter, M.L., Simon, J.-C.,
705 Speer, R., Stäker, J., Stein, R., Stöbel-Richter, Y., Stumvoll, M., Tarnok, A., Teren, A.,
706 Teupser, D., Then, F.S., Tönjes, A., Treudler, R., Villringer, A., Weissgerber, A.,
707 Wiedemann, P., Zachariae, S., Wirkner, K., Thiery, J., 2015. The LIFE-Adult-Study:
708 objectives and design of a population-based cohort study with 10,000 deeply phenotyped
709 adults in Germany. BMC Public Health 15, 691. doi:10.1186/s12889-015-1983-z
710 Lohmann, G., Margulies, D.S., Horstmann, A., Pleger, B., Lepsien, J., Goldhahn, D.,
711 Schloegl, H., Stumvoll, M., Villringer, A., Turner, R., 2010. Eigenvector centrality
712 mapping for analyzing connectivity patterns in fMRI data of the human brain. PLoS One
713 5, e10232. doi:10.1371/journal.pone.0010232
714 Mahinrad, S., Jukema, J.W., Van Heemst, D., MacFarlane, P.W., Clark, E.N., De Craen,
715 A.J.M., Sabayan, B., 2016. 10-Second heart rate variability and cognitive function in old
716 age. Neurology 86, 1120–1127. doi:10.1212/WNL.0000000000002499
717 Maier, S.U., Hare, T.A., 2017. Higher Heart-Rate Variability Is Associated with
718 Ventromedial Prefrontal Cortex Activity and Increased Resistance to Temptation in

719 Dietary Self-Control Challenges. J. Neurosci. 37, 446–455.
720 doi:10.1523/JNEUROSCI.2815-16.2017
721 Makovac, E., Garfinkel, S., Bassi, A., Basile, B., Macaluso, E., Cercignani, M., Calcagnini,
722 G., Mattei, E., Mancini, M., Agalliu, D., Cortelli, P., Caltagirone, C., Critchley, H.,
723 Bozzali, M., 2017. Fear processing is differentially affected by lateralized stimulation of
724 carotid baroreceptors. Cortex. 99, 200–212. doi:10.1016/j.cortex.2017.07.002
725 Marques, J.P., Kober, T., Krueger, G., van der Zwaag, W., Van de Moortele, P.F., Gruetter,
726 R., 2010. MP2RAGE, a self bias-field corrected sequence for improved segmentation
727 and T1-mapping at high field. Neuroimage 49, 1271–1281.
728 doi:10.1016/j.neuroimage.2009.10.002
729 Mather, M., Thayer, J.F., 2018. How heart rate variability affects emotion regulation brain
730 networks. Curr. Opin. Behav. Sci. 19, 98–104. doi:10.1016/j.cobeha.2017.12.017
731 McEwen, B.S., 2003. Interacting mediators of allostasis and allostatic load: Towards an
732 understanding of resilience in aging. Metabolism. 52, 10–16. doi:10.1016/S0026-
733 0495(03)00295-6
734 Molfino, A., Fiorentini, A., Tubani, L., Martuscelli, M., Fanelli, F.R., Laviano, A., 2009.
735 Body mass index is related to autonomic nervous system activity as measured by heart
736 rate variability. Eur. J. Clin. Nutr. 63, 1263–1265. doi:10.1038/ejcn.2009.35
737 Munoz, M.L., Van Roon, A., Riese, H., Thio, C., Oostenbroek, E., Westrik, I., De Geus,
738 E.J.C., Gansevoort, R., Lefrandt, J., Nolte, I.M., Snieder, H., 2015. Validity of (Ultra-
739)Short recordings for heart rate variability measurements. PLoS One 10, 1–15.
740 doi:10.1371/journal.pone.0138921
741 Nussinovitch, U., Elishkevitz, K.P., Kaminer, K., Nussinovitch, M., Segev, S., Volovitz, B.,
742 Nussinovitch, N., 2011a. The efficiency of 10-second resting heart rate for the evaluation
743 of short-term heart rate variability indices. PACE - Pacing Clin. Electrophysiol. 34,

744 1498–1502. doi:10.1111/j.1540-8159.2011.03178.x

745 Nussinovitch, U., Elishkevitz, K.P., Katz, K., Nussinovitch, M., Segev, S., Volovitz, B.,

746 Nussinovitch, N., 2011b. Reliability of ultra-short ECG indices for heart rate variability.

747 Ann. Noninvasive Electrocardiol. 16, 117–122. doi:10.1111/j.1542-474X.2011.00417.x

748 Porges, S.W., 2007. The polyvagal perspective. Biol. Psychol. 74, 116–143.

749 doi:10.1016/j.biopsycho.2006.06.009

750 Porges, S.W., 2001. The polyvagal theory: Phylogenetic substrates of a social nervous system.

751 Int. J. Psychophysiol. 42, 123–146. doi:10.1016/S0167-8760(01)00162-3

752 Porges, S.W., 1995. Orienting in a Defensive World. Psychophysiology.

753 Posner, J., Cha, J., Wang, Z., Talati, A., Warner, V., Gerber, A., Peterson, B.S., Weissman,

754 M., 2016. Increased Default Mode Network Connectivity in Individuals at High Familial

755 Risk for Depression. Neuropsychopharmacology 41, 1759–1767.

756 doi:10.1038/npp.2015.342

757 Power, J.D., Barnes, K.A., Snyder, A.Z., Schlaggar, B.L., Petersen, S.E., 2012. Spurious but

758 systematic correlations in functional connectivity MRI networks arise from subject

759 motion. Neuroimage 59, 2142–2154. doi:10.1016/j.neuroimage.2011.10.018

760 Raichle, M.E., MacLeod, A.M., Snyder, A.Z., Powers, W.J., Gusnard, D.A., Shulman, G.L.,

761 2001. A default mode of brain function. Proc. Natl. Acad. Sci. 98, 676–682.

762 doi:10.1073/pnas.98.2.676

763 Reitan, R.M., 1955. Certain differential effects of left and right cerebral lesions in human

764 adults. J Comp Physiol Psychol 48, 474–477.

765 Reitan, R.M., Wolfson, D., 1995. Category Test and Trail Making Test as Measures of

766 Frontal Lobe Functions. Clin. Neuropsychol. 9, 50–56.

767 doi:10.1080/13854049508402057

768 Rokem, A., Trumpis, M., Perez, F., 2009. Nitime: time-series analysis for neuroimaging data.

769 Proc. 8th Python Sci. Conf. (SciPy 2009) 1–8.

770 Sacchetti, B., Baldi, E., Lorenzini, C.A., Bucherelli, C., 2002. Cerebellar role in fear-
771 conditioning consolidation. Proc. Natl. Acad. Sci. 99, 8406–8411.
772 doi:10.1073/pnas.112660399

773 Sakaki, M., Yoo, H.J., Nga, L., Lee, T.-H., Thayer, J.F., Mather, M., 2016. Heart rate
774 variability is associated with amygdala functional connectivity with MPFC across
775 younger and older adults. Neuroimage 139, 44–52.
776 doi:10.1016/j.neuroimage.2016.05.076

777 Sin, N.L., Sloan, R.P., McKinley, P.S., Almeida, D.M., 2016. Linking Daily Stress Processes
778 and Laboratory-Based Heart Rate Variability in a National Sample of Midlife and Older
779 Adults. Psychosom. Med. 78, 573–582. doi:10.1097/PSY.0000000000000306

780 Singh, J.P., Larson, M.G., Tsuji, H., Evans, J.C., O'Donnell, C.J., Levy, D., 1998. Reduced
781 heart rate variability and new-onset hypertension: Insights into pathogenesis of
782 hypertension: The Framingham Heart Study. Hypertension 32, 293–297.
783 doi:10.1161/01.HYP.32.2.293

784 Smith, R., Thayer, J.F., Khalsa, S.S., Lane, R.D., 2017. The hierarchical basis of
785 neurovisceral integration. Neurosci. Biobehav. Rev. 75, 274–296.
786 doi:10.1016/j.neubiorev.2017.02.003

787 Streitbürger, D.P., Pampel, A., Krueger, G., Lepsien, J., Schroeter, M.L., Mueller, K., Möller,
788 H.E., 2014. Impact of image acquisition on voxel-based-morphometry investigations of
789 age-related structural brain changes. Neuroimage 87, 170–182.
790 doi:10.1016/j.neuroimage.2013.10.051

791 Swank, A.M., 1996. Physical Dimensions of Aging. Med. Sci. Sport. Exerc. 28, 398,399.
792 doi:10.1097/00005768-199603000-00018

793 Tarvainen, M.P., Niskanen, J.-P., Lipponen, J.A., Ranta-Aho, P.O., Karjalainen, P.A., 2014.

794 Kubios HRV--heart rate variability analysis software. Comput. Methods Programs
795 Biomed. 113, 210–220. doi:10.1016/j.cmpb.2013.07.024
796 Tataranni, P.A., Gautier, J.F., Chen, K., Uecker, A., Bandy, D., Salbe, A.D., Pratley, R.E.,
797 Lawson, M., Reiman, E.M., Ravussin, E., 1999. Neuroanatomical correlates of hunger
798 and satiation in humans using positron emission tomography. Proc. Natl. Acad. Sci. U. S.
799 A. 96, 4569–74. doi:http://dx.doi.org/10.1073/pnas.96.8.4569
800 Taubert, M., Lohmann, G., Margulies, D.S., Villringer, A., Ragert, P., 2011. Long-term
801 effects of motor training on resting-state networks and underlying brain structure.
802 Neuroimage 57, 1492–1498. doi:10.1016/j.neuroimage.2011.05.078
803 Thayer, J.F., Åhs, F., Fredrikson, M., Sollers, J.J., Wager, T.D., 2012. A meta-analysis of
804 heart rate variability and neuroimaging studies: Implications for heart rate variability as a
805 marker of stress and health. Neurosci. Biobehav. Rev. 36, 747–756.
806 doi:10.1016/j.neubiorev.2011.11.009
807 Thayer, J.F., Lane, R.D., 2007. The role of vagal function in the risk for cardiovascular
808 disease and mortality. Biol. Psychol. 74, 224–242. doi:10.1016/j.biopsycho.2005.11.013
809 Thayer, J.F., Lane, R.D., 2000. A model of neurovisceral integration in emotion regulation
810 and dysregulation. J. Affect. Disord. 61, 201–216. doi:10.1016/S0165-0327(00)00338-4
811 Thayer, J.F., Ruiz-Padial, E., 2006. Neurovisceral integration, emotions and health: An
812 update. Int. Congr. Ser. 1287, 122–127. doi:10.1016/j.ics.2005.12.018
813 Thayer, J.F., Sollers, J.J., Friedman, B.H., Koenig, J., 2015. Gender differences in the
814 relationship between resting heart rate variability and 24-hour blood pressure variability.
815 Blood Press. 7051, 1–5. doi:10.3109/08037051.2016.1090721
816 Thayer, J.F., Yamamoto, S.S., Brosschot, J.F., 2010. The relationship of autonomic
817 imbalance, heart rate variability and cardiovascular disease risk factors. Int. J. Cardiol.
818 141, 122–131. doi:10.1016/j.ijcard.2009.09.543

819 Uddin, L.Q., Kelly, A.M.C., Biswal, B.B., Castellanos, F.X., Milham, M.P., 2009. Functional
820 Connectivity of Default Mode Network Components: Correlation, Anticorrelation, and
821 Causality. Hum. Brain Mapp. 30, 625–637. doi:10.1002/hbm.20531
822 Umetani, K., Singer, D.H., McCraty, R., Atkinson, M., 1998. Twenty-four hour time domain
823 heart rate variability and heart rate: Relations to age and gender over nine decades. J.
824 Am. Coll. Cardiol. 31, 593–601. doi:10.1016/S0735-1097(97)00554-8
825 Voss, A., Schroeder, R., Heitmann, A., Peters, A., Perz, S., 2015. Short-term heart rate
826 variability - Influence of gender and age in healthy subjects. PLoS One 10, e0118308.
827 doi:10.1371/journal.pone.0118308
828 Wei, L., Chen, H., Wu, G.R., 2018. Heart rate variability associated with grey matter volumes
829 in striatal and limbic structures of the central autonomic network. Brain Res. 1681, 14–
830 20. doi:10.1016/j.brainres.2017.12.024
831 Williams, D.P., Cash, C., Rankin, C., Bernardi, A., Koenig, J., Thayer, J.F., 2015. Resting
832 heart rate variability predicts self-reported difficulties in emotion regulation: A focus on
833 different facets of emotion regulation. Front. Psychol. 6, 1–8.
834 doi:10.3389/fpsyg.2015.00261
835 Wink, A.M., de Munck, J.C., van der Werf, Y.D., van den Heuvel, O.A., Barkhof, F., 2012.
836 Fast Eigenvector Centrality Mapping of Voxel-Wise Connectivity in Functional
837 Magnetic Resonance Imaging: Implementation, Validation, and Interpretation. Brain
838 Connect. 2, 265–274. doi:10.1089/brain.2012.0087
839 Winkelmann, T., Thayer, J.F., Pohlack, S., Nees, F., Grimm, O., Flor, H., 2017. Structural
840 brain correlates of heart rate variability in a healthy young adult population. Brain Struct.
841 Funct. 222, 1061–1068. doi:10.1007/s00429-016-1185-1
842 Wong, S.W., Massé, N., Kimmerly, D.S., Menon, R.S., Shoemaker, J.K., 2007. Ventral
843 medial prefrontal cortex and cardiovagal control in conscious humans. Neuroimage 35,

698–708. doi:10.1016/j.neuroimage.2006.12.027

Yoo, H.J., Thayer, J.F., Greening, S., Lee, T.-H., Ponzio, A., Min, J., Sakaki, M., Nga, L., Mather, M., Koenig, J., 2017. Brain structural concomitants of resting state heart rate variability in the young and old: evidence from two independent samples. Brain Struct. Funct. doi:10.1007/s00429-017-1519-7

Yu, C., Zhou, Y., Liu, Y., Jiang, T., Dong, H., Zhang, Y., Walter, M., 2011. Functional segregation of the human cingulate cortex is confirmed by functional connectivity based neuroanatomical parcellation. Neuroimage 54, 2571–2581. doi:10.1016/j.neuroimage.2010.11.018

Zeki Al Hazzouri, A., Haan, M.N., Deng, Y., Neuhaus, J., Yaffe, K., 2014. Reduced heart rate variability is associated with worse cognitive performance in elderly Mexican Americans. Hypertension 63, 181–187. doi:10.1161/HYPERTENSIONAHA.113.01888

Zulfiqar, U., Jurivich, D.A., Gao, W., Singer, D.H., 2010. Relation of High Heart Rate Variability to Healthy Longevity. Am. J. Cardiol. 105, 1181–1185. doi:10.1016/j.amjcard.2009.12.022

860 **Supplementary Table 1.** Association (Spearman's rho) between heart rate variability (HRV)

861 and other parameters per age group.

	Young	Middle	Old
Age	-0.10	-0.21*	-0.01
mean FD (mm)	-0.13	-0.11	0.09
BMI (kg/m^2)	0.13	-0.20*	-0.14
WHR	-0.04	-0.17	-0.08
SBP (mmHg)	0.01	-0.17	-0.01
DBP (mmHg)	-0.06	-0.23*	-0.01
TMT A (s)	0.01	-0.12	-0.04
TMT B (s)	-0.06	-0.12	0.02

862 *$*p < 0.05$; $**p < 0.01$; $***p < 0.001$, 2-tailed.*

863 *Note.* FD = framewise displacement; BMI = body mass index; WHR = waist to hip ratio; SBP

864 = systolic blood pressure; DBP = diastolic blood pressure, TMT = trail making test.